An Ab Initio Study of the Hydrogen Chloride – Ammonia Complex

Gustavo Jorge Teixeira Tavares da Silva

Master's Degree in Chemistry

Department of Chemistry and Biochemistry of the Faculty of Sciences of the University of Porto

Advisor

Maria Natália Cordeiro, Associate Professor, Faculty of Sciences – University of Porto

Co-Advisor

Vesa Hänninen, Teaching Assistant, Faculty of Science – University of Helsinki

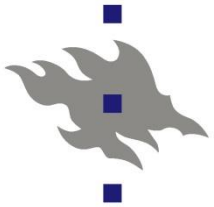

UNIVERSITY OF HELSINKI

U.PORTO

FACULDADE DE CIÊNCIAS
UNIVERSIDADE DO PORTO

Todas as correções determinadas pelo júri, e só essas, foram efetuadas.

O Presidente do Júri,

Porto, _____/_____/_____

Preface

The investigational study described was performed in the Laboratory of Physical Chemistry of the Department of Chemistry, University of Helsinki, which belongs to the Finnish Centre of Excellence in Physics, Chemistry, Biology, and Meteorology of Atmospheric Composition and Climate Change.

I want to express my deepest thanks to Prof. Lauri Halonen for the opportunity to work in a world renowned center and work with some of the best in the field. It was an amazing experience which I'm sure will be important for my future.

Also my sincere thanks to Vesa Häninen and Lauri Partanen, for their valuable advice, knowledge and help.

My earnest thanks to my advisor Maria Natália Cordeiro for her help, advice and incentive.

Special thanks for my friends Annina, Eetu, Luís, Matias and Nicola that were there with me and made my stay there a wonderful experience.

Finally, special thanks for my parents and my brother for all their support and always believing in me.

Abstract

The structure of ClH-NH_3 complex was investigated using the new CCSD(T)-F12a method with AVQZ basis set, corroborating previous results of a strong hydrogen bonded complex.

The harmonic vibration wavenumbers were also calculated with the same method, having obtained close results to the experimental for the ClH-NH_3 stretch (178 cm^{-1}) and for the NH_3 symmetric bending (1121 cm^{-1}), and other modes for which there are experimental results show the need for further refinement.

The H-Cl stretch is the mode showing the more discordance between the experimental (1371 cm^{-1}) and the calculated values (2390 cm^{-1}), after a anharmonic treatment using variational method, it showed a large improvement (2073 cm^{-1}), showing the importance of anharmonic treatment in this complex.

Also coupling effects were going to be taken in account but calculations weren't finalized.

Keywords: hydrogen chloride, ammonia, complex, CCSD(T)-F12a, structure, vibrations, harmonic, anharmonic

Resumo

A estrutura do complexo ClH-NH_3 foi investigada usando o novo método CCSD(T)-F12a com AVQZ basis set, corroborando resultados anteriores de um complexo com uma forte ponte de hidrogénio.

Também foram calculados os números de onda das vibrações harmónicas com o mesmo método, tendo obtido resultados próximos dos experimentais para o stretch ClH-NH3 (178 cm^{-1}) e para o bending simétrico do NH_3 (1121 cm^{-1}), outros modos para os quais existem dados experimentais mostram uma necessidade de refinação extra.

O stretch H-Cl é o modo que mostrou uma maior discrepância entre os resultados experimentais (1371 cm^{-1}) e os calculados (2390 cm^{-1}), após um tratamento anarmónico usando o método variacional, mostrou um grande melhoramento (2073 cm^{-1}), mostrando a importância do tratamento anarmónico neste complexo.

Efeitos de acoplamento eram também para terem sido tidos em conta, mas os cálculos não foram finalizados.

Palavras-chave: cloreto de hidrogénio, amoníaco, complexo, CCSD(T)-F12a, estrutura, vibrações, harmónicas, anarmónicas

Contents

Table Index

Figure Index

Abbreviations

AO – Atomic orbital

AVQZ – aug-cc-VQZ – Dunning augmented correlation-consistent polarized valence quadruple zeta basis set

CC – Coupled cluster

CCSD – Coupled Cluster with singles and doubles

CCSD(T) – Coupled Cluster with singles, doubles and pertubative triples

CGTO – Contracted Gaussian type orbitals

GTO – Gaussian type orbitals

HF – Hartree-Fock

IR – Infrared

MO – Molecular orbital

MP2 – Second order Møller-Plesset Many Body Pertubation Theory

PES – Potential energy surface

RHF – Restricted Hartree-Fock

SCF-MO – Self-consistent field molecular orbital

STO – Slater type orbitals

Symbols

ϵ_0 – Vacuum permittivity

h – Planck's constant

$\hbar$ – Reduced Planck's constant

μ – Reduced mass

Other symbols might have more than one meaning depending on the equation they are being used, they are all opportunely described.

1. Introduction

In the field of atmospheric sciences The H_3N-HCl complex has been considered a prototype system for investigation of particle formation from volatile species.[1, 2] Furthermore, it's an interesting study system due to being a simple model representation for proton transfer reactions, which are essential for many biological processes.

Even before there was any experimental evidence of a stable H_3N-HCl complex, Mulliken, in 1952, proposed that two possible stable structures could occur [3]: an H-bonded-like complex and a more stable ion-pair-like separated by an energy barrier. To check these hypotheses Clementi *et al.* carried out ab initio self-consistent field molecular orbital (SCF-MO) calculations and thermodynamics analyses in 1967 and uncovered that, within the restricted Hartree-Fock (RHF) scheme a single bound complex described the potential energy surface of HCl approaching NH_3 lacking any barrier amid the separated fragments and the complex [4,5].

The first experimental confirmation of complex formation has been acquired from mass spectroscopic studies by Verhaegen and Goldfinger [6], and corroboration on the H-bonded nature of the complex was obtained by Pimentel by examining the complex infrared (IR) spectra at 15 K in a nitrogen matrix [7].

Recently there were important advances in the different explicitly correlated methods that take in account the singularities in potential energy at points were two electrons overlap [8-12]. Particularly, the explicitly correlated Coupled Cluster (CC) method with perturbative triples and some additional approximations to the explicitly correlated treatment, CCSD(T)-F12a, turned possible to obtain very accurate electronic energies and equilibrium structures with only a small increase in computational time than necessary in standard CCSD(T) methods [12,13].

The purpose of this study is to accurately calculate the equilibrium structure and vibrational frequencies of the H_3N-HCl complex. The CCSD(T)-F12a method was chosen to be employed along with the Dunning augmented correlation-consistent polarized valence quadruple zeta basis set (aug-cc-VQZ) [14-16]. The results were then compared to the existing experimental data and some previous works.

1.1. Hydrogen chloride

Hydrogen chloride (chemical formula HCl) is a colorless gas at room temperature. It's a diatomic molecule composed of one hydrogen atom and one chlorine atom. Due to the chlorine atom being a lot more electronegative than the hydrogen atom, the covalent bond between the two atoms is quite polar, thus the molecule has a large dipole moment. Because of its acidic nature, HCl is corrosive. One of the main functions of HCl in atmosphere is as a reservoir species for chlorine [17,18].

Table 1 - Main sources of atmospheric chlorine [19-21].

Source	%
Manmade (CFC's and related)	~80
CH_3Cl (mostly natural)	15-20
Inorganic Sources (*e.g.* volcanoes)	>5

The main sources of chlorine are shown in Table 1. Chlorine is important in atmospheric studies due to triggering a catalytic loss mechanism for O_3 that involves cycling between Cl and ClO (also known as the ClO_x cycle):

$$Cl + O_3 \rightarrow ClO + O_2 \quad \textbf{(1)}$$

$$ClO + O \rightarrow Cl + O_2 \quad \textbf{(2)}$$

The catalytic cycle is only terminated with the conversion of the active chlorine into its reservoir species. For mid latitude, lower stratosphere, HCl and $ClONO_2$ are the dominant reservoir species for chlorine constituting over 90% of the total inorganic chlorine (Figure 1). They are converted according to the equations:

$$Cl + CH_4 \rightarrow HCl + CH_3 \quad \textbf{(3)}$$

$$ClO + NO_2 \xrightarrow{M} ClONO_2 \quad \textbf{(4)}$$

Hydrogen chloride is relatively stable and some fraction of it migrates back to the troposphere and is removed from it by precipitation. Hydrogen chloride has a lifetime of a few weeks.

Chlorine nitrate is also relatively unreactive but is not actually removed from the atmosphere. Chlorine nitrate is an especially important species because it store two catalytic agents, NO_2 and ClO. The lifetime for chlorine nitrate is around one day.

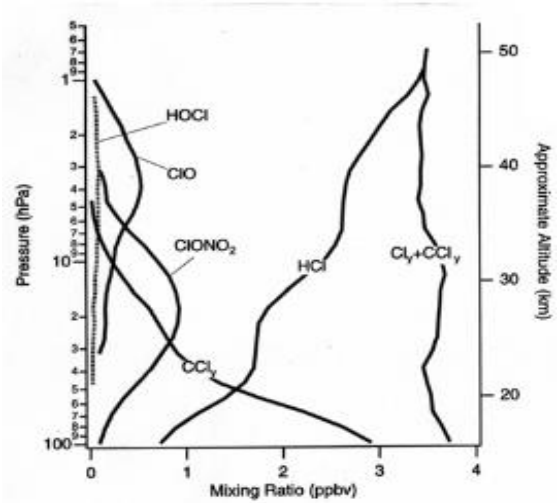

Figure 1 - Measurements of the major components of stratospheric chlorine versus pressure [17].

These species can return to an active state through the reactions:

$$HCl + OH \rightarrow Cl + H_2O \quad \textbf{(5)}$$

$$ClONO_2 \xrightarrow{h\upsilon} \begin{cases} Cl + NO_3 \\ ClO + NO_2 \end{cases} \quad \textbf{(6)}$$

This cycle is one among others that govern stratospheric ozone chemistry. Any process that even modestly shifts the balance away from reservoir species to ClO can have a large impact in ozone depletion.

A few other reactions HCl that can participate under stratospheric conditions are [18]:

$$ClONO_2 + HCl \rightarrow Cl_2 + HNO_3 \quad \textbf{(7)}$$

$$N_2O_5 + HCl \rightarrow ClNO_2 + HNO_3 \quad \textbf{(8)}$$

$$HOCl + HCl \rightarrow Cl_2 + H_2O \quad \textbf{(9)}$$

$$HO_2NO_2 + HCl \rightarrow HOCl + HNO_3 \quad \textbf{(10)}$$

1.2. Ammonia

Ammonia is a compound of nitrogen and hydrogen with the chemical formula NH_3. Ammonia is the main basic gas in the atmosphere and, after N_2 (nitrogen gas) and N_2O (nitrous oxide), the most abundant nitrogen containing compound in the

atmosphere. Some significant sources of ammonia are animal waste, ammonification of humus with subsequent emission from soils, losses of ammonia based fertilizers from soils and industrial emissions [17]. The estimated ammonia emission can be seen in Table 2.

Table 2 - Estimated annual global ammonia emissions [17].

Source	Amount[a] / Tg N yr^{-1}
Agricultural (domestic animals, synthetic fertilizers, crops)	37.4
Natural (oceans, undisturbed soils, wild animals)	10.7
Biomass burning	6.4
Other (humans and pets, industrial processes, fossil fuels)	3.1
Total	57.6

[a] Expressed as tera-grams of nitrogen per year.

Because ammonia is readily absorbed by surfaces such as water and soil, its residence time in lower atmosphere is likely to be quite short, around ten days. Wet and dry deposition of ammonia are the main mechanisms of atmospheric removal for ammonia. Its deposition may represent an important nutrient to the biosphere in some areas due to its importance as a source of nitrogen. Atmospheric concentrations of ammonia are quite variable being dependent on the proximity of a rich source of ammonia [17,18].

Ammonia reacts rapidly with both sulfuric and nitric acids to form fine particles:

$$NH_3 + H_2SO_4 \rightarrow NH_4HSO_4 \quad \textbf{(11)}$$

$$NH_3 + NH_4HSO_4 \rightarrow (NH_4)_2SO_4 \quad \textbf{(12)}$$

$$NH_3 + HNO_3 \leftrightarrow NH_4NO_3 \quad \textbf{(13)}$$

Ammonia reaction with sulfuric acid or ammonium bisulfate is favored over the reaction with nitric acid.

2. Quantum Chemical Principles

The wavefunction Ψ completely defines the states of a system in quantum chemistry. In other words, the energies, particle locations and all other physical proprieties can be determined from the wavefunction. Generally quantum chemical calculations revolve around the discovery of the wavefunction and then finding the wanted properties. By solving the system's Schrödinger equation we obtain its wavefunction:

$$\hat{H}\Psi = \mathrm{i}\hbar\frac{\partial\Psi}{\partial t}, \tag{14}$$

where $\hat{H}$ is the system's Hamiltonian, that is to say its energy operator, $\hbar$ is the Planck's constant *h* divided by 2π and i is the imaginary unit. The wavefunction depends on the locations of all particles in the system and time $\Psi = \Psi(x_1, x_2, \dots, x_n, t)$.

Frequently we are concerned about systems in which the probabilistic features of the wavefunction are time invariant, *i.e.* they do not vary with time. Equation (14) can be divided into different parts that characterize the time and space variations of Ψ in these stationary states. As a result it becomes possible to partition the wavefunction into its space and time components $\Psi = \psi(x_1, x_2, \dots, x_n)\tau(t)$, where the time dependence is simply $\tau(t) = \exp(-iEt/\hbar)$ and *E* is the system's energy [22]. The time-independent Schrödinger equation has the following form in this notation:

$$\hat{H}\psi = E\psi. \tag{15}$$

In core, it is the eigenvalue equation of the system's energy. Not taking in account the relativist effects [23], the Hamiltonian operator in equation (15) is made of the operators for kinetic and potential energy, which can be written off as:

$$\hat{H} = \hat{K} + \hat{V} = -\sum_{i=1}^{N}\frac{\hbar^2}{2m_i}\nabla_i^2 + \frac{1}{4\pi\epsilon_0}\sum_{i=1}^{N}\sum_{j<i}^{N}\frac{q_i q_j}{r_{ij}}, \tag{16}$$

in Cartesian coordinates for a system of N charged particles, where q_i and q_j are the charges of the particles under consideration, r_{ij} is the distance between them, m_i is the mass of the particle i and ϵ_0 is the vacuum permitivity.

This second order differential equation can only be solved analytically for a system with two particles, and so it's necessary to use numerical methods to obtain the wavefunctions for larger systems. We have to use to a number of approximations in order to make the numerical solution of the equation (15) possible, amongst which are the Born-Oppenheimer and adiabatic approximations.

2.1. The Born-Oppenheimer and Adiabatic Approximations

The nuclear mass is around three to four times higher in magnitude than the electronic mass, so we can assume that the electrons respond instantaneously to changes in nuclear configuration, while the nucleus only feel an average potential linked to the electron movement. This lets us separate the time scale of both movements. This separation is achieved in the following manner: In a system of N_e electrons and N_n nuclei, in a center of mass coordinate system, the Hamiltonian equation (16) can be represented in the form [23-25]

$$\hat{H} = \hat{K}_n + \hat{K}_e + \hat{V}_{ne} + \hat{V}_{ee} + \hat{V}_{nn} + \hat{H}_{mp} = \hat{K}_n + \hat{H}_e + \hat{H}_{mp} \quad \textbf{(17)}$$

where $\hat{K}_n$ and $\hat{K}_e$ are the nuclear and electronic kinetic energy operators, respectively, $\hat{V}_{ne}$ is the potential energy term between the electrons and the nuclei, $\hat{V}_{ee}$ is the potential energy term between electrons, and $\hat{V}_{nn}$ is the nuclear potential energy term. In the right side of the equation, the electron dependent terms have been united to form the electronic Hamiltonian operator $\hat{H}_e$. As it is impossible to separate center of mass motion from internal motion in a system of more than two particles, that is why it results in the appearance of the mass-polarization operator $\hat{H}_{mp}$.

Since the electronic Hamiltonian is Hermitian, the electronic wavefunctions $\psi_{e,i}(y,x)$ that are solution to the Schrödinger equation:

$$\hat{H}_e \psi_{e,i}(y,x) = E_i(y)\psi_{e,i}(y,x) \quad \textbf{(18)}$$

form a complete orthonormal set of functions. In equation (18) y are the nuclear coordinates and x are the electron coordinates, and E_i is the energy eigenvalue of the electronic Hamiltonian for the state $\psi_{e,i}$. Both the wavefunctions and the energies

depend on the location of the nuclei, this arises as a consequence of the nuclear coordinates entering $\hat{H}_e$ as parameters that define $\hat{V}_{ne}$ and $\hat{V}_{nn}$.

The completeness of the $\psi_{e,i}$ set means that it is possible to express the wave functions of the total Hamiltonian as a linear combination of the electronic wavefunctions:

$$\psi = \sum_{i=1}^{\infty} \psi_{n,i}(y)\psi_{e,i}(y,x), \tag{19}$$

where $\psi_{n,i}(y)$ are the expansion coefficients, which turn out to be the nuclear wavefunctions.

The nuclear wavefunctions can be found by operating on this function with the total Hamiltonian of equation (17), multiplying from the right by a specific $\psi_{e,k}$ and integrating over all space. This results in the following equation [23]:

$$\begin{aligned} E_{tot}\psi_{n,k} &= \hat{K}_n\psi_{n,k} + E_k\psi_{n,k} \\ &+ \sum_{i=1}^{\infty}\left(2\langle\psi_{e,k}|\nabla_n|\psi_{e,i}\rangle\nabla_n + \langle\psi_{e,k}\left|\hat{K}_n\right|\psi_{e,i}\rangle + \langle\psi_{e,k}\left|\hat{H}_{mp}\right|\psi_{e,i}\rangle\right)\psi_{n,i,} \end{aligned} \tag{20}$$

with the operator ∇_n being defined by the equation:

$$\nabla_n^2 = \hat{K}_n = -\sum_{j=1}^{N_n}\frac{\hbar^2}{2m_{a,j}}\nabla_j^2, \tag{21}$$

with $m_{a,j}$ being the atomic mass associated with the nuclei j, and:

$$\nabla_j^2 = \left(\frac{\partial^2}{\partial X^2}, \frac{\partial^2}{\partial Y^2}, \frac{\partial^2}{\partial Z^2}\right). \tag{22}$$

In equation (20), the terms under summation represent the coupling between different electronic states. The first two terms inside the parenthesis are known as the first and second order non-adiabatic coupling elements. The adiabatic approximation sets these coupling terms equal to zero, leaving only the terms for which $i = k$. It is valid in systems where the reaction takes place on a single potential energy surface, and fails for example when the reaction contains spin-forbidden transitions, as in many photochemical reactions [23,26].

Since the mass-polarization operator depends inversely on the total mass of the molecule an additional approximation can be made. Due to the electron mass being much smaller than the total mass the mass-polarization term is negligible in most cases.

Taking in account this approximations and the fact that the first non-adiabatic couplings are zero for all except spatially degenerate wavefunctions [23], from equation (20) we obtain:

$$E_{tot}\psi_{n,k} = \left(\widehat{K}_n + E_k + \langle\psi_{e,k}|\widehat{K}_n|\psi_{e,k}\rangle\right)\psi_{n,k}. \quad \textbf{(23)}$$

In the Born-Oppenheimer approximation the diagonal correction terms $\langle\psi_{e,k}|\widehat{K}_n|\psi_{e,k}\rangle$ are set to zero, resulting from an equation in the form:

$$E_{tot}\psi_{n,k}(y) = \widehat{K}_n\psi_{n,k}(y)E_k(y)\psi_{n,k}(y). \quad \textbf{(24)}$$

According to equation (24), the nucleic motion follows a potential energy surface $E_i(y)$ that can be acquired by solving the electronic Schrödinger equation.

The Born-Oppenheimer approximation works for most systems, but is unsuccessful when two states of the system become energetically very close. The errors resulting from the Born-Oppenheimer approximation are frequently very small and they are largest in systems containing the hydrogen nuclei [23,27]. Even so in a hydrogen fluoride molecule, for example, the Born-Oppenheimer approximation only introduces a shift of 1.5 cm^{-1} in the harmonic wavenumber [28].

The electronic Schrödinger equation retains the general form of (15) with the Born-Oppenheimer approximation, and for a system consisting of N_e electrons and N_n nuclei, the electronic Hamiltonian can be written as:

$$\widehat{H} = -\frac{\hbar^2}{2m_e}\sum_{i=1}^{N_e}\nabla_i^2 - \frac{1}{4\pi\epsilon_0}\sum_{i=1}^{N_e}\sum_{k=1}^{N_n}\frac{q_k e}{r_{ik}} + \frac{1}{4\pi\epsilon_0}\sum_{i=1}^{N_e}\sum_{i<j}^{N_e}\frac{e^2}{r_{ij}} \quad \textbf{(25)}$$

with the potential energy being split into two terms, one related to the nuclear electron-attractions, and the other with electron-electron repulsions.

Although the Born-Oppenheimer approximation is the essential approximation lying beneath almost all ab initio calculations, for systems comprising more than one electron it is impossible to solve equation (25) exactly and additional approximations are necessary.

2.2. The Hartree-Fock Approach

The electron-electron interaction term in equation (25) creates some difficulties in the Schrödinger equation solution. One way is to treat this interaction as an approximation, in a way that each electron is traveling in the average field created by all the other electrons and the nuclei, this is the Hartree-Fock (HF) approach. The origins of this method are within the variational method, which states that for any trial wavefunction (ψ_t) the Rayleigh ratio ($\mathcal{E}$), defined as [23]:

$$\mathcal{E} = \frac{\langle \psi_t | \hat{H} | \psi_t \rangle}{\langle \psi_t | \psi_t \rangle}, \tag{26}$$

is always greater or equal to the system energy E. So the variational theorem declares that there is a lower border to the energy attained from our trial wavefunction that is, at all times, larger or equal to the true energy.

Since the electronic wavefunction has to fulfill the Pauli principle, it is sound to take the trial Hartree-Fock wavefunction (Φ_0) in the form of a Slater determinant:

$$\Phi_0 = \frac{1}{\sqrt{N_e!}} det|\varphi_a(1)\varphi_b(2)\varphi_c(3) \dots \varphi_z(N_e)|, \tag{27}$$

with $\varphi_a, \varphi_b, \varphi_c \dots \varphi_z$ denoting molecular orbitals. Frequently in equation (27) the one electron wavefunctions are called spinorbitals. The spinorbitals can be acquired by multiplying the spatial orbital with the spin part of the wavefunction in the absence of an external field [29]. Habitually each spinorbital is expanded as a linear combination of a set of n basis functions (ξ_p):

$$\varphi_u = \sum_{p=1}^{n} c_{pu} \xi_p, \tag{28}$$

where c_{pu} are the coefficients we need to determine. Worth noting that from this set of basis functions exactly n linearly independent wavefunctions can be made.

With the electronic Hamiltonian and the trial wavefunction defined by equations (25) and (27), the variational theorem tells us that the obstacle in the Hartree-Fock calculations is now minimizing the energy functional $\langle \Phi_0 | \hat{H} | \Phi_0 \rangle$ under the limitation that the different spinorbitals must remain orthonormal. This is done by

using the method of Lagrange multipliers, and it outcome is a series of Hartree-Fock equations of the type [23,30]:

$$\hat{f}_i\big|\varphi_u(i)\rangle = \epsilon_u|\varphi_u(i)\rangle, \quad \textbf{(29)}$$

where the Fock operator is defined as:

$$\hat{f}_i = \hat{h}_i + \sum_{u=a}^{z}\Big(\hat{J}_u(i) - \hat{K}_u(i)\Big), \quad \textbf{(30)}$$

where the sum is over the occupied molecular orbitals and ϵ_u are orbital energies. In equation (30) $\hat{h}_i$ is a one electron core Hamiltonian:

$$\hat{h}_i = -\frac{\hbar^2}{2m_e}\nabla_i^2 - \frac{1}{4\pi\epsilon_0}\sum_{j=1}^{N_n}\frac{q_j e}{r_{ij}}, \quad \textbf{(31)}$$

which is made of the kinetic energy of the electron and its interactions with the nuclei. For the electrons i and j the Coulomb operator ($\hat{J}_u(i)$) is defined by the integral:

$$\hat{J}_u(i)\big|\varphi_u(i)\rangle = \frac{e^2}{4\pi\epsilon_0}\langle\varphi_u(j)|\frac{1}{r_{ij}}|\varphi_u(j)\rangle\,|\varphi_u(i)\rangle. \quad \textbf{(32)}$$

The Coulomb operator accounts for the Coulombic repulsions between electrons. $\hat{K}_u(i)$ is called the exchange operator and it is described by the integral:

$$\hat{K}_u(i)\big|\varphi_v(i)\rangle = \frac{e^2}{4\pi\epsilon_0}\langle\varphi_v(j)|\frac{1}{r_{ij}}|\varphi_v(j)\rangle\,|\varphi_v(i)\rangle. \quad \textbf{(33)}$$

The exchange operator takes in account some sort of correlation on the motion in space of pairs of electrons, it is also known as Fermi correlation.

The spinorbitals emerging in equation (29) are not the same as those transpiring in equation (27), but instead linear combinations labeled canonical spinorbitals. This doesn't cause any computational difficulty because the transformation between the two sets of spinorbitals is unitary, and in a unitary transform the determinant's total wavefunction is left unaffected.

By inserting equation (28) and multiplying from the left by $\langle\xi_q|$, the Fock equations for al orbitals are transformed into a matrix equation:

$$\boldsymbol{FC = SCE}, \quad \textbf{(34)}$$

where $\boldsymbol{C}$ is an $n \times n$ matrix of the coefficients and $\boldsymbol{E}$ is an $n \times n$ diagonal matrix of the orbital energies. The elements in the Fock matrix ($\boldsymbol{F}$) have the form:

$$F_{qp} = \langle \xi_q(i) | \hat{f}_i | \xi_p(i) \rangle, \quad \textbf{(35)}$$

and the elements in the overlap matrix ($\boldsymbol{S}$):

$$S_{qp} = \langle \xi_q(i) | \xi_p(i) \rangle. \quad \textbf{(36)}$$

Fundamentally the problem of determining the best possible determinant's wavefunction has been converted into a problem of finding the coefficient matrix. Linear algebra tells us that the matrix equation (34) can have a non-trivial solution only if the condition:

$$det|\boldsymbol{F} - \epsilon_u \boldsymbol{S}| = 0 \quad \textbf{(37)}$$

is fulfilled. We start by giving it an initial set of coefficients and then calculate the Fock and overlap matrices from equations (35) and (36), respectively. From these, a new set of orbital energies and coefficients are acquired that can then be used to recalculate the Fock and overlap matrices and so on, creating an iterative process. Normally the cycle is repeated until the difference between the new and old coefficients is insignificant and the system has reached self-consistency. The variational theorem in equation (26) warranties that the final energies are always greater than the true energy of the system independently of the choice of the basis functions.

2.3. Electron Correlation

The Hartree-Fock method accounts for 99% of the total energy, regrettably this remaining 1% is crucial when dealing with chemical phenomena. This difference between the Hartree-Fock energy and the lowest possible energy for a given basis function arises from the instantaneous Coulombic and spin correlation effects, which cause the electrons to evade each other more than what the average Hartree-Fock treatment suggests, and is called the electron correlation [23,30,31].

Electron correlation can be classified in a small number of ways. It can be separated into static and dynamic correlation, with static correlation signifying the

more stable kind of correlation between electrons that are distant from each other, *i.e.* in different spatial orbitals, and dynamic correlation being the immediate correlation amongst two electrons that occupy the same spatial orbital. An alternative division is between Fermi and Coulomb correlation, where Fermi correlation is the correlation amid same spin electrons and Coulomb correlation is between opposite spin electrons.

Since the Hartree-Fock method provides the best one-determinantal wavefunction Φ_0 as its answer for the ground state wavefunction, supplementary determinants have to be considered if electron correlation is to be taken into account. These determinants can be constructed from the leftover $n - N_e$ virtual orbitals that result from filling the lowest of our n spinorbitals with N_e electrons. The several types of excited determinants $\Phi_1, \Phi_2, \ldots$ are created by promoting electrons to the virtual orbitals φ_α. As an example if we think in a case of two electron excitement from spinorbitals b and c in equation (27) to the virtual orbitals φ_α and φ_β, we would have one of the doubly exited determinants:

$$\Phi_{bc}^{\alpha\beta} = \frac{1}{\sqrt{N_e!}} det\left|\varphi_a \varphi_\alpha \varphi_\beta \ldots \varphi_z\right|. \quad \textbf{(38)}$$

These determinants, or small linear combinations of them assembled to reach the correct electron symmetry, are eigenfunctions of all the operators that commute with $\widehat{H}$ and are known as configuration state functions. Conditional on the actual electron correlation approach, the actual wavefunction is then characterized as some sort of linear combination of the different configuration state functions.

Some usual techniques to deal with electron correlation are Configuration Interaction, Møller-Plesset Many Body Pertubation Theory, and Coupled Cluster.

2.4. Coupled Cluster Methods

Coupled Cluster is a numerical technique used for describing many-body systems.

The method was originally developed in the 1950s for the study of nuclear physics phenomena, but turn out to be more frequently used when in 1966 the method was reformulated for tackling electron correlation in atoms and molecules.

It starts from the Hartree-Fock molecular orbital method and adds a correction term to take into account electron correlation. This is done by taking in account all orders of electron excitations up to a given type. To accomplish this, we need the assistance of the cluster operator $\hat{T}$ defined by the equation [23,30]:

$$\hat{T} = \hat{T}_1 + \hat{T}_2 + \cdots + \hat{T}_{Ne}, \tag{39}$$

where $\hat{T}_n$ are excitation operators. The $\hat{T}_n$ produce a set of excited determinants of a given order n after operating on the Hartree-Fock wavefunction. As an example, a $\hat{T}_2$ operating on the Hartree-Fock wavefunction outcomes in a series of determinants of the shape:

$$\hat{T}_2\Phi_0 = \sum_{u<v}^{occ}\sum_{\alpha<\beta}^{vir} t_{uv}^{\alpha\beta}\Phi_{uv}^{\alpha\beta}, \tag{40}$$

and it's customary to call amplitudes to the expansion coefficients t. The Coupled Cluster wavefunction is defined as:

$$\begin{aligned}\psi_{CC} = e^{\hat{T}}\Phi_0 &= \left(1 + \hat{T} + \frac{1}{2!}\hat{T}^2 + \frac{1}{3!}\hat{T}^3 + \cdots\right)\Phi_0 \\ &= \left[1 + \hat{T}_1 + \left(\hat{T}_2 + \frac{1}{2}\hat{T}_1^2\right) + \left(\hat{T}_3 + \hat{T}_2\hat{T}_1 + \frac{1}{3!}\hat{T}_1^3\right) + \cdots\right]\Phi_0\end{aligned} \tag{41}$$

The first term creates the reference Hartree-Fock and the second the entire singly excited states. The first parenthesis generates all doubly exited states, which can be considered connected ($\hat{T}_2$) or disconnected ($\hat{T}_1^2$). The second parenthesis produces completely the triply exited states, these can be "true" ($\hat{T}_3$) or "product" ($\hat{T}_2\hat{T}_1$, $\hat{T}_1^3$) triples. Physically a connected type as $\hat{T}_3$ corresponds to three electrons interacting simultaneously with each other, while a disconnected term like $\hat{T}_2\hat{T}_1$ describes the interaction between a pair of non-interacting electrons and a lone

electron. Since it turns out to be increasingly improbable to have a large number of electrons interacting at the same time, it can be presumed that the significance of the $\hat{T}_k$ terms declines as k increases.

Using the whole Taylor expansion up to $\hat{T}_{Ne}$ would yield all the correlation energy for the given basis set, nevertheless for systems all but the smallest systems this is impossible and the series must be truncated. Due to the Brillouin's theorem the Coupled Cluster that involves only singles excitations would return the Hartree-Fock energy. So the lowest improvement we can do is by treating only the double excitations that account for two electron excitations. Complementing with the singles has little influence on the computational effort (n^6 scaling) and to some extent improves the outcomes by introducing orbital relaxation. Adding the triples increases the computational scaling to n^8 and consequently can only be used for small systems [23].

In theory there are two ways to calculate the Coupled Cluster energy from the Hamiltonian equation:

$$\hat{H}e^{\hat{T}}\Phi_0 = E_{CC}e^{\hat{T}}\Phi_0. \quad \textbf{(42)}$$

The first would be to use the variational theorem (26) by choosing $\psi_t = e^{\hat{T}}\Phi_0$. Solutions of this category have strong advantages, as in addition to being variational they can be used in systems with strong electron correlations where the second method fails [32]. Alas, due equation (41) displaying factorial complexity even for truncated $\hat{T}$, the variational solution is only realistic in very small systems.

In the standard method, the Coupled Cluster Schrödinger equation is projected to the reference wavefunction Φ_0 by multiplying the right side of equation (42) with $\langle\Phi_0|$. This produces the correlation energy expression [23]:

$$E_{CC} = \langle\Phi_0|\hat{H}e^{\hat{T}}|\Phi_0\rangle$$
$$= E_0 + \sum_{u<v}^{occ}\sum_{\alpha<\beta}^{vir}\left(t_{uv}^{\alpha\beta} + t_u^{\alpha}t_v^{\beta} + t_u^{\beta}t_v^{\alpha}\right)\left[(\varphi_\alpha\varphi_u|\varphi_\beta\varphi_v) - (\varphi_\beta\varphi_u|\varphi_\alpha\varphi_v)\right]. \quad \textbf{(43)}$$

From equation (43) we can see that the energy depends only on two-electron molecular orbital integrals and singles and doubles amplitudes.

The undetermined amplitudes can be discovered by projecting the Schrödinger equation onto space spanned by the exited determinants. Normally this is done through a similarity transformation of the Hamiltonian, which can be obtained from equation (42) by multiplication from the left with $e^{-\hat{T}}$:

$$e^{-\hat{T}}\hat{H}e^{\hat{T}}\Phi_0 = E_{CC}\Phi_0. \quad \textbf{(44)}$$

After this, a set of algebraic equations for the coefficients can be acquired by multiplication from the left with $\langle\Phi_u^\alpha|, \langle\Phi_u^\alpha|$, etc. These equations can be solved by iterative methods and from the coefficients in the energy in (43) can be estimated [23,33].

As said earlier, since the Coupled Cluster with singles and doubles (CCSD) method scales at n^6 and the addition of higher excitations causes a rise in computation effort that is of two orders of magnitude per level, CCSD is usually the only reasonable pure Coupled Cluster technique for large systems. Yet, due to the small size of the $\hat{T}_1$ terms, most of the influence from triple excitations results from the $\hat{T}_3$ term in (41). This term can be employed into standard CCSD by using perturbation theory. In the most successful formulation of the different perturbational methodologies, denoted CCSD(T) and presented by Raghavachari et al. [34], the $\hat{T}_3$ term is estimated by a fourth order Møller–Plesset calculation with the original CCSD amplitudes and added to the final energy [35]. Even though this method increases the computational scaling to n^7, due to its consistently good results CCSD(T) has emerged as the so-called “gold standard” method of modern computational chemistry [36-38].

Recently, it has been understood that including a small number of terms that depend explicitly on the interelectronic distance in the wavefunction could improve the slow convergence of the electronic correlation energy [39]. It has been shown that the newly developed explicitly correlated CCSD(T)-F12 method using a triple-ζ basis set provide better results than a conventional CCSD(T) with a quintuple-ζ basis set [40-42].

2.4.1. CCSD(T)-F12 and F12a Methods

In equation (25) the electron-electron interaction terms origin singularities in the potential energy, which leads into cusps in the wavefunction at points where two electrons coincide. Due to the need of the kinetic energy to annul the infinity of the potential energy, this outcomes in the wavefunction behaving linearly around the points r_{ij} [23]. The majority of the convergence difficulties in the standard methods arise from the detail that the slowly varying orbital product form $\varphi_u(r_i)\varphi_v(r_j)$ is unfit for describing the cusp when the electrons i and j are nearby each other.

To circumvent this problem the CCSD(T)-F12 and F12a methods by Adler *et al.* [18] define the wavefunction as:

$$\left|\psi_{CCSD(T)-F12}\right\rangle = e^{(\hat{T}_1+\hat{T}_2)}|\Phi_0\rangle. \quad \textbf{(45)}$$

Using Einstein summation rule, where summation over repeated indexes is implicit, the cluster operators $\hat{T}_1$ and $\hat{T}_2$ are defined as:

$$\hat{T}_1 = t_\alpha^u \hat{C}_u^\alpha \quad \textbf{(46)}$$

$$\hat{T}_2 = \frac{1}{2} T_{\alpha\beta}^{uv} \hat{C}_{uv}^{\alpha\beta} + \frac{1}{2} \mathcal{T}_{RS}^{uv} \hat{C}_u^R \hat{C}_v^S, \quad \textbf{(47)}$$

where $\hat{C}_u^R$, $\hat{C}_{uv}^{\alpha\beta}$ are one and two electron excitation operators, the first of which defines an excitation into a formally complete virtual space $\{R, S, \dots\}$. It follows from the completeness of this space that it can be partitioned into the union $\{R, S, \dots\} = \{\alpha, \beta, \dots\} \cup \{X, Y, \dots\}$ where $\{X, Y, \dots\}$ is a complementary auxiliary basis set. Equation (46) and the first term on the right in equation (47) characterize the standard first and second order excitations to virtual orbitals as in equation (41).

The additional amplitudes $\mathcal{T}_{RS}^{uv}$ can be found from equations:

$$\mathcal{T}_{RS}^{uv} = T_{mn}^{uv} \mathcal{F}_{RS}^{mn} \quad \textbf{(48)}$$

$$\mathcal{F}_{RS}^{mn} = \left\langle \varphi_m \varphi_n \middle| F_{12} \hat{Q}_{12} \middle| \varphi_R \varphi_S \right\rangle, \quad \textbf{(49)}$$

where T_{mn}^{uv} are the amplitudes used in the F12 handling and m and n denote some occupied orbitals. F_{12} is the short-range correlation factor concerning electrons one and two. The most intuitive choice of setting $F_{12} = r_{12}$, done initially by Kutzelnigg and Klopper [8,43,44], it is not the ideal pick when using comparatively small basis sets

of double zeta or triple zeta quality [10]. Instead it has been shown by Tew and Klopper [9] that the preeminent correlation factor comes in the form of a Slater function, which can be additionally matched to a set of Gaussian geminals [45] to make computations easier:

$$F_{12} = \frac{1}{\gamma} e^{-\gamma r_{12}} \approx \sum_k c_k e^{-a_k r_{12}^2}, \tag{50}$$

where the coefficients c_k and a_k are uncovered by least squares fitting [46] and γ is a parameter.

The projector operator $\hat{Q}_{12}$ in equation (49) guarantees that the different F12 configurations

$$\left|\Phi_{uv}^{mn}\right\rangle = \mathcal{F}_{RS}^{mn} \hat{C}_u^R \hat{C}_v^S |\Phi_0\rangle \tag{51}$$

are orthogonal with the configurations attained from the standard MO basis. It has the form:

$$\hat{Q}_{12} = (1 - \hat{o}_1)(1 - \hat{o}_2)(1 - \hat{v}_1 \hat{v}_2), \tag{52}$$

where $\hat{o}_i = |\varphi_u(i)\rangle\langle\varphi_u(i)|$ projects on the occupied subspace and $\hat{v}_i = |\varphi_\alpha(i)\rangle\langle\varphi_\alpha(i)|$ projects on the virtual subspace. Taking in account definitions (48), (49), (51) and (52) the terms $\mathcal{F}_{RS}^{mn}$ can be understood as contraction coefficients between the larger set of configurations $|\Phi_{uv}^{RS}\rangle$ and the smaller $|\Phi_{uv}^{mn}\rangle$ one.

In summary, the additional amplitudes are there to introduce new functions into the conventional CC expansion where the products $|\varphi_u(1)\varphi_v(2)\rangle$ have been swapped with a negative short-range correlation function:

$$|\chi_{uv}(1,2)\rangle = T_{mn}^{uv} \hat{Q}_{12} F_{12} |\varphi_m(1)\varphi_n(2)\rangle. \tag{53}$$

This not only reduces the probability of encountering two electrons in the same position, but also improves the performance of the wave function in the neighborhood of the cusp. The most vital terms in (53) are the ones for which $mn = uv$ or $mn = vu$. By disregarding less essential terms in the wavefunctions $T_{mn}^{uv}|\Phi_{uv}^{mn}\rangle$, it is possible to simplify calculations [12]. In this fixed amplitude scheme, the amplitudes T_{mn}^{uv} in the wavefunction are set to zero for all terms except T_{uu}^{uu}, T_{uv}^{uv} and T_{vu}^{uv}, which are assigned fixed values so that the wavefunction satisfies the cusp conditions. The benefits of this kind of fixed amplitude ansatz are that it is unitary invariant, free of germinal basis set superposition error and size consistent [47].

As in conventional CCSD equations, in CCSD-F12, the energy and amplitude are calculated by multiplying from the left with a suitable configuration. The energy is found by the multiplication of $|\Phi_0\rangle$, same as in CCSD. In the case of the amplitudes the multiplication of the contravariant configurations:

$$\left|\widetilde{\Phi}_u^{\alpha}\right\rangle = \frac{1}{2}\hat{C}_u^{\alpha}|\Phi_0\rangle \tag{54}$$

$$\left|\widetilde{\Phi}_{uv}^{\alpha\beta}\right\rangle = \frac{1}{6}\left(2\hat{C}_{uv}^{\alpha\beta} - \hat{C}_{vu}^{\alpha\beta}\right)|\Phi_0\rangle \tag{55}$$

results in equations for the single and double residuals:

$$R_{\alpha}^{u} = \left\langle\widetilde{\Phi}_u^{\alpha}\middle|\widehat{H} - E\middle|\psi_{CCSD(T)-F12}\right\rangle \tag{56}$$

$$R_{\alpha\beta}^{uv} = \left\langle\widetilde{\Phi}_{uv}^{\alpha\beta}\middle|\widehat{H} - E\middle|\psi_{CCSD(T)-F12}\right\rangle. \tag{57}$$

The best values for the coefficients are then obtained by forcing both equations (56) and (57) to be equal to zero. As a consequence of the fixed T_{mn}^{uv} amplitudes, the number of equations is unchanged from the standard CCSD formulation. The equations are different due to the extra terms related to the explicitly correlated terms. Some of these new terms can be simplified by the use of the resolution of identity [12].

The more complicated doubles residual of equation (57) can be characterized in matrix form in the basis of the virtual orbitals (α, β) as [12,48]:

$$\boldsymbol{R}_{CCSD-F12}^{uv} = \boldsymbol{R}_{MP2-F12}^{uv} + \boldsymbol{K}(\mathcal{D}^{uv}) + \boldsymbol{K}(\mathcal{T}^{uv}) + \alpha_{uv,kl}\boldsymbol{D}^{kl} + \boldsymbol{G}^{uv} + \boldsymbol{G}^{vu\dagger}, \tag{58}$$

where k and l run over occupied orbitals. The first term on the right is the MP2-F12 residual, and is given by the equation [46]:

$$\boldsymbol{R}_{MP2-F12}^{uv} = \boldsymbol{K}^{uv} + \boldsymbol{F}\boldsymbol{T}^{uv} + \boldsymbol{T}^{uv}\boldsymbol{F} - F_{uk}\boldsymbol{T}^{kv} - \boldsymbol{T}^{uk}F_{kv} + \boldsymbol{C}^{mn}T_{mn}^{uv}, \tag{59}$$

where $\boldsymbol{T}^{uv}$ are amplitude matrices, the terms $F_{rs} = \left\langle\varphi_r\middle|\hat{f}\middle|\varphi_s\right\rangle$ are blocks of the closed shell Fock matrix, with the Fock operator $\hat{f}$ defined by equation (30) and $K_{\alpha\beta}^{uv} = \left(\varphi_\alpha\varphi_u\middle|\varphi_\beta\varphi_v\right)$ are the usual interchange integrals. The r and s in the Fock matrix element refer to any orbital representative in the AO basis. All the anomalies arising from the explicitly correlated terms are assimilated in the last term of equation (59) which styles the coupling to the explicitly correlated configurations. In the F12 method it is guessed as [12,46]:

$$C_{\alpha\beta}^{uv} = F_{\alpha X}\left\langle\varphi_X\varphi_\beta\middle|F_{12}\middle|\varphi_u\varphi_v\right\rangle + \langle\varphi_\alpha\varphi_X|F_{12}|\varphi_u\varphi_v\rangle F_{X\beta}. \tag{60}$$

The second term in equation (58) is the external exchange operator. It includes all contractions of the doubles amplitudes that involve three or four virtual orbitals and is in the form:

$$[\boldsymbol{K}(\mathcal{D}^{uv})]_{\alpha\beta} = \big(\varphi_\alpha\varphi_r\big|\varphi_\beta\varphi_s\big)\mathcal{D}_{rs}^{uv}, \tag{61}$$

where $\mathcal{D}_{rs}^{uv}$ are composite amplitude matrices, for which $\mathcal{D}_{\gamma\eta}^{uv} = T_{\gamma\eta}^{uv} + t_\gamma^u t_\eta^v$, $\mathcal{D}_{k\eta}^{uv} = \delta_{ku} t_\gamma^v$, $\mathcal{D}_{\gamma k}^{uv} = \delta_{vk} t_\gamma^u$ and $\mathcal{D}_{kl}^{uv} = 0$. The greek letters γ and η refer to virtual orbitals.

The adjustments to $\boldsymbol{K}(\mathcal{D}^{uv})$ created from the added explicitly correlated terms establish the third term. With the help of equation (48) the elements of this matrix can be written as:

$$[\boldsymbol{K}(\mathcal{T}^{uv})]_{\alpha\beta} = V_{\alpha\beta}^{mn} T_{mn}^{uv}, \tag{62}$$

where:

$$V_{\alpha\beta}^{mn} = \big\langle \varphi_\alpha\varphi_\beta\big|r_{12}^{-1}\hat{Q}_{12}F_{12}\big|\varphi_m\varphi_n\big\rangle. \tag{63}$$

Using the resolution of identity, this three electron integral can be written as [11,13]:

$$\begin{aligned} V_{\alpha\beta}^{mn} = \left\langle \varphi_\alpha\varphi_\beta\left|\frac{F_{12}}{r_{12}}\right|\varphi_m\varphi_n\right\rangle &- \big(\varphi_\alpha\varphi_r\big|\varphi_\beta\varphi_s\big)\langle\varphi_r\varphi_s|F_{12}|\varphi_m\varphi_n\rangle \\ &- \big(\varphi_\alpha\varphi_u\big|\varphi_\beta\varphi_X\big)\langle\varphi_u\varphi_X|F_{12}|\varphi_m\varphi_n\rangle \\ &- \big(\varphi_\alpha\varphi_X\big|\varphi_\beta\varphi_u\big)\langle\varphi_X\varphi_u|F_{12}|\varphi_m\varphi_n\rangle. \end{aligned} \tag{64}$$

The $\boldsymbol{K}(\mathcal{T}^{uv})$ terms have the largest impact, besides the $\boldsymbol{R}_{MP2-F12}^{uv}$ term, on the amplitudes because they are the only terms that have contractions of doubles amplitudes with integrals over three or four orbitals [12].

Finally in equation (58) we have the terms $\alpha_{uv,kl}$ and $\boldsymbol{G}^{uv}$. These are intermediates that depend on amplitudes and integrals with at most two external orbitals. The external-external block matrices have the elements $[\boldsymbol{D}^{uv}]_{\alpha\beta} = \mathcal{D}_{\alpha\beta}^{uv}$.

The holdup of the CCSD(T)-F12 calculation is the coupling of the new correlated terms with the original CCSD amplitudes. A straight application of the CCST(T)-F12 method shown rises the computational effort by an order of magnitude compared with the standard CCSD(T). In a way to circumvent that the CCSD(T)-F12a [13] uses some approximations, the most significant consists of ignoring all contributions of the explicitly correlated configurations to $\boldsymbol{R}_{CCSD-F12}^{uv}$ with the exception of $\boldsymbol{K}(\mathcal{T}^{uv})$ and the coupling matrices $\boldsymbol{C}^{mn}$ in equation (59). Likewise due to the small

value, as revealed by small density procedures [49] and numerical estimation [12], of the tricky last two terms of in equation (64) involving integrals over two virtual orbitals and one complementary auxiliary orbital and be consequently ignored. With this in mind the $V_{\alpha\beta}^{mn}$ terms are easily described as:

$$\begin{aligned} V_{\alpha\beta}^{mn} &= W_{\alpha\beta}^{mn} - K(F^{mn})_{rs} \\ &= \left\langle \varphi_r \varphi_s \left| \frac{F_{12}}{r_{12}} \right| \varphi_m \varphi_n \right\rangle - \left(\varphi_r \varphi_x \middle| \varphi_y \varphi_s\right) \left\langle \varphi_x \varphi_y \middle| F_{12} \middle| \varphi_m \varphi_n \right\rangle, \end{aligned} \tag{65}$$

where x and y are some orbitals representable in the atomic orbital basis. As a consequence of the equal form of the last term in equation (65) and the external exchange operators, the total residual of the CCSD(T)-F12a method shortens to:

$$\begin{aligned} \boldsymbol{R}_{CCSD-F12}^{uv} = \boldsymbol{R}_{MP2-F12}^{uv} + \overline{\boldsymbol{C}}^{uv} + \overline{\boldsymbol{W}}^{uv} + \boldsymbol{K}(\mathcal{D}^{uv} - \bar{\mathcal{F}}^{uv}) \\ + \alpha_{uv,kl} \boldsymbol{D}^{kl} + \boldsymbol{G}^{uv} + \boldsymbol{G}^{vu\dagger} \end{aligned} \tag{66}$$

where $\bar{\mathcal{F}}^{uv} = F_{rs}^{mn} T_{mn}^{uv}$ and the terms $\bar{W}_{rs}^{uv}$ and $\bar{C}_{\alpha\beta}^{uv}$ are defined in the same fashion.

After the amplitudes are known, the energies can be calculated. Next the perturbative triples are carried as in CCSD(T) method and their energy is added to the F12 energy [12].

As a consequence of all the approximations, the CCSD(T)-F12a scales formally like the CCSD(T) method, nonetheless it gives much more accurate results. With minimal extra computational effort, calculations performed at the aug-cc-pVDZ level provide results as good as calculations performed with the CCSD(T)/aug-cc-pVQZ level, whereas an aug-cc-pVTZ basis set performs as well as at a CCSD(T)/aug-cc-pV5Z level [12,13,50]. The method decreases by an order of magnitude basis set errors of atomization energies, reaction energies, electron affinities, ionization potentials, equilibrium structures and vibrational frequencies [12]. Analogous benefits have been validated for equilibrium structures and anharmonic vibrational frequencies of large molecules [51]. The cancelation of errors concerning overestimating the F12 correlation energies and underestimating the non-corrected triples contributions are perhaps the reason these small basis perform so well [12]. Yet, due to this cancellation being extremely systematic, the results are trustworthy to a high accuracy.

2.5. Basis Functions

In computational chemistry, besides the chosen method, another important choice is the set of basis functions, as this choice will influence the computational costs, and the accuracy, and so have a big impact on the results.

The two principal types of basis functions, are the Slater type orbitals [52] (STO) and the Gaussian type orbitals [53] (GTO). STOs are composed of an exponentially decreasing radial dependence multiplying the angular part of the analytic hydrogen-like orbitals $Y_{l,m}(\theta,\phi)$ [54]:

$$\xi^{s}_{nlm}(r,\theta,\phi) = Nr^{n-1}e^{-\zeta}Y_{l,m}(\theta,\phi), \quad \textbf{(67)}$$

with N being a normalization constant and ζ is a parameter typically obtained by fitting the STOs to numerically computed atomic orbitals [30]. The variables (r,θ,ϕ) are given in spherical coordinates for the quantum numbers l and m, $l \in \mathbb{N}$ and $m \in \mathbb{Z}$. Equation (67) ensues that the Slater type orbitals have no radial nodes except for the one located at origin, so a radial nodal structure can only be constructed by using a linear combination of STOs. The use of STOs is harshly restricted by the fact that the numerous three- and four-center two electron integrals required by practically all correlation methods cannot be analytically calculated with them. As a result of this inconvenience the Slater type orbitals are only exploitable for the smallest systems that need very high accuracy or that can overlook the problematic integrals completely [23].

The Gaussian type orbitals are described by [30]

$$\xi^{g}_{ijk}(x,y,z) = (x-x_c)^i(y-y_c)^j(z-z_c)^k e^{-\zeta|r-r_c|^2}, \quad \textbf{(68)}$$

where the point $r_c = (x_c, y_c, z_c)$ defines the center of the Gaussian function and the parameter ζ determines how fast the GTO declines. As in STOs the parameter ζ is determined with variational calculations with atoms [55]. In most cases the centers of the GTOs corresponds to the nuclei in the system. The parameters $\{i,j,k\} \in \mathbb{N}$ term the amount of nodes the Gaussian function includes, moreover their sum categorizes the GTO as s, p, d, etc. From equation (68) we can infer that the multiplication of two Gaussian functions is another Gaussian function [56], this causes an increase in

computation efficiency due to the abundant two electron integrals encountered in the diverse correlation methods.

The shortcomings of the GTOs are that because of their r^2 dependence in the exponential term, they regularly decay too quickly matched to the actual wavefunctions, furthermore they have a zero slope at the center of the Gaussian. Taking those problems in account the GTOs usually give a worse depiction of the orbitals, and so a larger basis set is needed to reach equivalent accuracy. In spite of this, the negative characteristics of the GTOs are hugely surpassed by the increased efficiency in integral calculations. The GTOs are the most widespread type of basis function used in quantum chemistry.

Due to the large contribution of the core electrons to the system energy, the variational calculations employed to determine the set of parameters ζ for a set of GTO-basis functions usually offer biased outcomes since the resulting functions are predominantly optimized around them [23]. To bypass this problem, a set of primitive Gaussian functions of equation (68) centered at the same point are often grouped together with Gaussian contractions (CGTO) of the form:

$$\xi_p^g = \sum_l d_{lp} \xi_l^g, \tag{69}$$

where the coefficients d_{lp} are predetermined and so remain constant during the actual variational calculation.

Since the unchanging core orbitals can be described by a single contraction and don't need to be reevaluated at every cycle of iteration, the employment of CGTO causes the computations to be a lot cheaper. Most of the modern high accuracy calculations apply basis sets where the contraction is general, meaning that most of the primitives enter any given contracted Gaussian function but with different contraction coefficients for different CGTOs [57]. After the contraction, a linear combination of the atom centered CGTO is used to represent the spatial orbitals of the system as in equation (28) and the coefficients are determined by the Hartree-Fock calculation.

The number of basis functions unsurprisingly hangs on the needed accuracy and complexity of the system. Each of the atomic orbitals in the elementary valence theory is described, in the smallest basis set, by one function only. The Double Zeta

(DZ) -type sets double the number of basis functions, but for many systems is essential to go beyond to Triple, Quadruple or even Quintuple Zeta basis set, with three, four and five times the basis functions of the smallest basis, respectively. It is widespread the application of split valence basis sets where the number of basis functions is multiplied only for the valence electrons, since the computational effort with many of the correlation methods increases swiftly with the basis set size. This tactic is acceptable as the inner shells are practically independent of the chemical environment of the system.

When using correlation methods, oftentimes only summing more functions of the same type to a given basis doesn't meaningfully enhance the computational results. That is due to the functions being incapable to account for the distortion of the atomic orbitals instigated by neighboring atoms and for the angular correlation arising from situations where electrons are in the opposite sides of the nucleus [23]. By adding polarization functions, which are functions with higher value of angular momentum, this problem can be dealt with.

It's advantageous if the change from a basis set to a more complete one increases the percentage of recovered correlation energy in some predictable way. This is accomplished in the correlation consistent (cc) basis sets of Dunning [14,15], where angular momentum functions with an alike energy contribution are inserted jointly as the basis approaches completeness. As an example, instead of inserting all the d functions into the basis at once, the cc basis sets add the polarization functions in the succession 1d, 2d1f, 3d2f1g [58].

The use of correlation consistent basis sets also causes it to theoretically feasible to reach the complete basis limit, that is, the correlation energy if the basis set used to expand the wave function was infinite. This is accomplished by doing calculations with an increasing quantity of basis functions and then extrapolating the results to the basis set limit. This method isn't doable in large systems considering that the majority of the extrapolation formulae often have three or more parameters [23,59,60], and so a calculation of at least the correlation consistent quadruple zeta basis set is compulsory.

In case the system includes hydrogen bonding or strong van der Walls interactions it is required to further polish the basis set by adding diffuse functions.

Diffuse functions decay slowly with increasing distance from the Gaussian center due to having a small value of the exponential coefficient ζ in equation (68). These functions are added to the augmented correlation consistent (aug-cc) variant of the Dunning cc-basis set [61].

Besides the correlation consistent basis sets described above, other prevalent basis sets are Ahlrich type basis sets, Pople style basis sets and Dunning and Huzinaga basis sets [23].

2.6. Solutions to the Nuclear Hamiltonian

2.6.1. Geometry Optimization

We'll now look at the solution of the Nuclear Hamiltonian of equation (24). Since the equilibrium geometry relates to a global energy minimum of the potential energy surface, the geometry optimization converts into uncovering the minimum energy. Nearly all the methods to pinpoint that minimum energy take advantage of the fact that for an alteration in nucleus position $\boldsymbol{y} - \boldsymbol{y}_0$, the variation in energy can be described as a Taylor series:

$$E(\boldsymbol{y}) = E(\boldsymbol{y}_0) + \left(\frac{\partial E}{\partial \boldsymbol{y}}\right)^T (\boldsymbol{y} - \boldsymbol{y}_0) + \frac{1}{2}(\boldsymbol{y} - \boldsymbol{y}_0)^T \frac{\partial^2 E}{\partial \boldsymbol{y}^2}(\boldsymbol{y} - \boldsymbol{y}_0) + \cdots, \quad \textbf{(70)}$$

where the first derivative is the gradient vector, which points in the direction of the maximum increase in energy, the second derivative is a matrix of the harmonic force constants and higher derivatives are anharmonic corrections to the vibrational frequencies. The power T denotes transpose vector.

Using equation (70) we can classify the different algorithms for locating the minima. The simplest methods make use only of the energies and are the slowest to converge, nonetheless they are worthwhile when the calculation of derivatives is not possible for some reason. The simplex algorithm is a well-known example of this kind of method. Algorithms that make use of not only the energies but also include the first derivative are one order of magnitude more efficient. Widespread examples are the steepest descents method and the conjugate gradients minimization. Finally the most

efficient and accurate algorithms employ the energies and both first and second derivatives. An example of a second-derivative method is the Newton-Rhapson method [30,55].

2.6.2. Harmonic Wavenumbers

For a deviance from equilibrium with the coordinates $\boldsymbol{y}_e$ the first derivative of equation (70) disappears due to the stationary nature of $\boldsymbol{y}_e$. By setting the zero of potential energy to be $E(\boldsymbol{y}_e)$ and disregarding all terms of third and higher order in equation (70), substitution into the Schrödinger equation (24) gives:

$$\left[-\sum_{j=1}^{3N_n}\left(\frac{1}{2m_{a,j}}\frac{\partial^2}{\partial y_j^2}\right)+\frac{1}{2}(\boldsymbol{y}-\boldsymbol{y}_e)^T\frac{\partial^2 E}{\partial \boldsymbol{y}^2}(\boldsymbol{y}-\boldsymbol{y}_e)\right]\psi_n = E_n\psi_n. \quad \textbf{(71)}$$

This equation can then be transformed into mass-dependent coordinates $z_j = \sqrt{m_{a,j}}(y_j - y_{e,j})$:

$$\left[-\sum_{j=1}^{3N_n}\left(\frac{1}{2}\frac{\partial^2}{\partial z_j^2}\right)+\frac{1}{2}(\boldsymbol{z})^T(\boldsymbol{F}\cdot\boldsymbol{G})(\boldsymbol{z}_e)\right]\psi_n = E_n\psi_n \quad \textbf{(72)}$$

with the $\boldsymbol{G}$ matrix defined by $G_{j,k} = 1/\sqrt{m_{a,j}m_{a,k}}$ and $\boldsymbol{F}$ is a $3N_n \times 3N_n$ matrix of the force constants $(\partial^2 E/\partial z^2)$. Lastly, a unitary transformation $\boldsymbol{U}$ is used to diagonalize the $\boldsymbol{F}\cdot\boldsymbol{G}$ matrix. With a coordinate change, $q = Uz$, the Schrödinger equation is transformed into a set of $3N_n$ one-dimensional harmonic oscillator equations [23]:

$$\left[-\sum_{j=1}^{3N_n}\left(\frac{1}{2}\frac{\partial^2}{\partial q_j^2}+\frac{1}{2}\varepsilon_j q_j^2\right)\right] = E_n\psi_n. \quad \textbf{(73)}$$

From the eigenvalues of the unitary transformation ε_j, the harmonic frequencies are calculated $\nu_j = \sqrt{\varepsilon_j}/2\pi$ and the eigenvectors $\boldsymbol{q}$ are the mass-weighed coordinates. Once the frequencies are known, the wavenumbers can be calculated, $\bar{\upsilon}_j = \upsilon_j/c$ where c is the speed of light in vacuum.

In theory, for a nonlinear molecule six of the $3N_n$ eigenvalues should be zero (for a linear molecule would be five). In spite of this, since the equilibrium geometry is

always merely an estimate and the gradient isn't a true zero, the six degrees of freedom corresponding to the translations and rotations of the molecule have to be projected out of the calculations [23]. The physical understanding of the normal modes is that they match to somehow secluded motions of groups of atoms in the sense that each normal mode can be exited without exiting any other modes.

Using an accurate potential energy surface (PES), the harmonic frequencies are likely to overestimate the experimental ones by about 5% due to the absence of higher-order terms in equation (71). Also, significant errors are instigated by the missing correlation contributions because of the truncation of both the one-electron and N_e-electron basis sets [62].

2.6.3. Anharmonic Wavenumbers

The harmonic approximation performs the best in systems in which the potential curve is properly approximated by a second order polynomial. As a consequence, in systems with a single deep minimum, the harmonic approximation can be employed for the few lowest frequencies with some accuracy. For higher vibrational quantum numbers v doesn't perform so well since the equally spaced harmonic ladder is unsuccessful in the description of the ever increasing density of vibrational states as the dissociation limit becomes closer. In cases where there are multiple potential energy minima, the splitting of states instigated by tunneling effects makes the harmonic approximation to fail completely. For these cases the higher order derivatives of equation (70) can't be overlooked, and consequently the division into several normal coordinates isn't as advantageous as before.

The dimensionality of the PES increases as the system increases with a rate of three for each added atom. Unfortunately the complete anharmonic handling involves calculations of huge areas of this PES, and so it is only doable for small systems. For a single water molecule with its three vibrational degrees of freedom, the complete anharmonic handling is feasible employing the same general methods as in the solution of the electron correlation problem. It's possible to circumvent this problem by dividing large systems into smaller uncoupled sub-systems that can then

be handled with higher accuracy. As in the approach taken by Kauppi and Halonen [63], after the PES calculation the vibrational problem was solved variationally.

For the variational calculation the nuclear Hamiltonian was expressed in terms of curvilinear coordinates. With the omission of angular momentum components in the Hamiltonian, it can be articulated in the form [63,64]:

$$\hat{H} = \hat{T} + \hat{V} = -\frac{h^2}{2}\sum_{ij}\left[\left(\frac{\partial g^{(q_i,q_j)}}{\partial q_i}\right)\frac{\partial}{\partial q_j} + g^{(q_i,q_j)}\frac{\partial^2}{\partial q_i \partial q_j}\right] + \hat{V}'(\boldsymbol{q}) + \hat{V}(\boldsymbol{q}), \qquad \textbf{(74)}$$

where $\boldsymbol{q}$ are the curvilinear internal coordinates and $g^{(q_i,q_j)}$ are the elements of the mass-weighed reciprocal matrix and have the form [64]:

$$g^{(q_i,q_j)} = \sum_{\alpha}^{N_n}\frac{1}{m_\alpha}(\nabla_\alpha q_i)\cdot(\nabla_\alpha q_j) \qquad \textbf{(75)}$$

with m_α being the masses of the nuclei. $\hat{V}'(\boldsymbol{q})$ is a small pseudopotential operator which is independent from the momentum operators [65,66] and is of quantum mechanical origin. Lastly, $\hat{V}(\boldsymbol{q})$ is the potential energy operator given in curvilinear internal coordinates.

The main benefits from curvilinear coordinates are that they present a more accurate characterization of the potential energy surface and make the potential energy surface parameters independent of the isotopes within the Born-Oppenheimer approximation [65]. The biggest problem with the curvilinear coordinates is that the kinetic energy operator turns out to be more complex in curvilinear coordinates as seen on equation (74).

From equation (74) the eigenvalues were obtained variationally. A basis set of harmonic oscillator wavefunctions $\xi^h(x)$ of the type [54]:

$$\xi_n^h(x) = \left[\frac{1}{n!\,2^n\pi^{\frac{1}{2}}}\left(\frac{\mu k}{\hbar^2}\right)^{\frac{1}{4}}\right]^{\frac{1}{2}} e^{-\left(\frac{\mu k}{\hbar^2}\right)^{\frac{1}{2}}\left(\frac{x^2}{2}\right)} H_n\left[\left(\frac{\mu k}{\hbar^2}\right)^{\frac{1}{4}}x\right] \qquad \textbf{(76)}$$

was used, were $\mu = \frac{m_1 m_2}{m_1+m_2}$ is the reduced mass of the system, k is the force constant and H_n is a hermite polynomial:

$$H_n(x) = (-1)^n e^{x^2} \frac{d^n}{dx^n}\left(e^{-x^2}\right). \quad \textbf{(77)}$$

Morse oscillator wavefunctions of the form [67]:

$$\xi_n^m(x) = N e^{\frac{\lambda}{2} e^{-\alpha(x-x_0)}} \left(\lambda e^{-\alpha(x-x_0)}\right)^{\frac{\lambda-2n-1}{2}} L_n^{\lambda-2n-1}\left(\lambda e^{-\alpha(x-x_0)}\right) \quad \textbf{(78)}$$

were also used. N is a normalization constant defined as:

$$N = n! \left[\frac{\alpha(\lambda-2n-1)}{\Gamma(n+1)\Gamma(\lambda-n)}\right]^{\frac{1}{2}}, \quad \textbf{(79)}$$

α is the Morse shape parameter, λ is defined as:

$$\lambda = \frac{2(2\mu V_0)^{\frac{1}{2}}}{\alpha\hbar}, \quad \textbf{(80)}$$

were V_0 is the depth of the well potential. In equation (78) L is the Laguerre polynomial which can be represented as:

$$L_n^v(x) = \frac{e^x x^{-v}}{n!} \frac{d^n}{dx^n}\left(x^{v+n} e^{-x}\right). \quad \textbf{(81)}$$

In the normalization constant formulation (79) the Γ are the Gamma function.

3. Results and Discussion

3.1. Geometry Optimization and Energies

Initially, it is necessary to determine the equilibrium structure of the complex. In this study that was done in two stages. First using data from literature [69] a CCSD(T)-F12a calculation with the Dunning [14,15,61] aug-cc-pVTZ basis set was performed. This calculation was then refined using the same method with a higher quality aug-cc-pVQZ basis set. Because the F12 method greatly decreases basis set superposition errors [12,70], the counterpoise correction was not used in this study. All geometry optimizations, single point calculations and frequency calculations were carried out with the MOLPRO suit of programs [71].

In Table 3, the total energies are reported obtained with both basis sets. Since the result with aug-cc-pVQZ shows an improvement in energy, all further calculations were done with that basis.

Table 3 - The CCSD(T)-F12a total energies.

basis	Energy (Hartrees)
aug-cc-pVTZ	-516.87721
aug-cc-pVQZ	-516.88708

The optimized geometry of ClH-NH_3 indicates the form of a hydrogen bonded complex with the HCl and NH_3 subunits geometries approximately the same as individual HCl and NH_3 molecules as can be seen on Table 4. This is consistent with the microwave experiments [72,73] and previous ab initio calculations [69,74]. The complex shows C_{3v} symmetry as expected. The hydrogen bond distance, r(N···H_b), is shorter than more typical hydrogen-bonded system

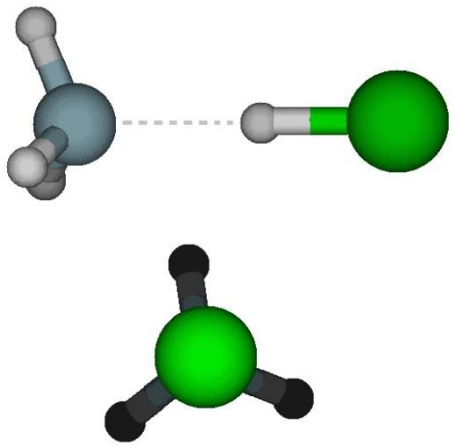

Figure 2 - Views from different perspectives of the optimized structure.

such as water dimer (1.96 Å), indicating a strong hydrogen bond between HCl and NH_3. The heavy atom distance, r(N···Cl), is in agreement with the experimental data, but it should be noted here that the experimental geometry values correspond to the molecules in the ground vibrational state, and those aren't exactly the same as the equilibrium values obtained in geometry optimization. The close agreement with the experimental values and high level computational methods can be attributed to the fact that the vibrational effects are small for small molecules.

Table 4 - Intermolecular distances (Å) and bond angles (degrees).

parameter	MP2 6-311++G(d,p) [69]	CCSD(T)-F12a aug-cc-pVQZ	Experimental ClH-NH_3 [73]	Experimental HCl [75]	Experimental NH_3 [76]
r(H—Cl)	1.312	1.320	—	1.275	—
r(N···H_b)	1.820	1.797	—	—	—
r(N—H)	1.016	1.012	—	—	1.012
r(N···Cl)	3.132	3.118	3.136	—	—
∠ HNH_b	112.1	111.6	—	—	—
∠ HNH	106.7	107.3	—	—	106.7
∠ NHCl	180.0	180.0	—	—	—

3.2. Harmonic Vibrational Wavenumbers

Harmonic wavenumbers were calculated on the CCSD(T)-F12a/AVQZ level.

The first observation of the infrared ClH-NH_3 spectrum is due to Pimentel [7] who observed in a N_2 matrix a H-Cl stretching frequency at 750 cm^{-1} and a H-Cl bending frequency of 605 cm^{-1}. Later, Barnes *et al.* [77] reported a more complete set of fundamentals, observed in Ar and N_2 matrices, in that work it was shown that the infrared spectrum of the ClH-NH_3 complex is extremely sensitive to the environment, and that the enormous shifts in the H-Cl stretching frequency upon complexation are partly due to proton transfer induced by the matrix. It was also shown that this phenomenon is particularly large in N_2 matrices, and the authors concluded that the ClH-NH_3 species in an Ar matrix is probably a better approximation to the isolated

complex. For this reason the experimental values reported in Table 5 report only experimental data for the complex relative to measurements in argon matrices.

Table 5 - Harmonic Vibration Frequencies (in cm^{-1}) [a].

mode	Assignment	CCSD(T)-F12a aug-cc-pVQZ	Experimental		
			$ClH\text{-}NH_3$ [77]	HCl [78]	NH_3 [78]
υ_1	NH_3 asym s	3613	3420		3444
υ_2	NH_3 asym s	3613	"		"
υ_3	NH_3 sym s	3481	—		3337
υ_4	HCl s	2390	1371	2886	
υ_5	NH_3 asym b	1671	—		1627
υ_6	NH_3 asym b	1671	—		"
υ_7	NH_3 sym b	1121	1072		950
υ_8	HCl b, NH_3 wag	750	1289		
υ_9	HCl b, NH_3 wag	750	"		
υ_{10}	HCl b, NH_3 rock	223	733		
υ_{11}	HCl b, NH_3 rock	222	"		
υ_{12}	N-HCl s	178	166		

[a] " denotes degenerate vibration modes; s=stretching; b=bending; wag=wagging; rock=rocking; sym=symmetric; asym=asymmetric.

The NH_3 asymmetric stretching is affected by the complexation, this effect is both seen in the experimental and the calculated values, conversely the experimental and the calculated values differ in the shift direction, showing the experimental a decrease in frequency and the calculated an increase. The calculated values are nonetheless in agreement with the direction of the shift that was calculated in previous works [69,79], so there might be some anharmonic and/or matrix effects on these vibrations. The symmetric stretching shows only a small effect from the complexation, but there are no experimental values to compare with, probably due to a small infrared intensity of this mode. Very little effect is also experienced by the asymmetric bending modes, but the symmetric bending mode experiences an increase in frequency that is also shown in the experimental values.

The shift created by the complexation in the HCl stretching frequency is vital in this vibrational analysis, given that is directly connected with the position of the hydrogen atom between the chlorine and nitrogen atoms and to the shape of the potential energy around it. The experimental values shown in Table 5 report a

dramatic shift for the HCl stretching frequency, indicating a decrease slightly larger than 1500 cm^{-1}, this isn't reproduced in any computational calculation [69,70,80,81], and on this calculation the shift is just under 500 cm^{-1}, confirming the presence of matrix effects influencing the results. Those are probably also the cause of the large difference between the calculated and the experimental frequencies of the other intermolecular motions with the exception of the N-HCl stretch. For this last mode there is a good agreement between the calculated and the experimental frequency value.

To further refine the HCl stretch and make sure it wasn't anharmonic effects causing the large difference between the experimental and the calculated frequencies an anharmonic study of that vibration was performed.

3.3. Anharmonic Vibrational Wavenumbers

For all these single point calculations, the CCSD(T)-F12a was also used with the AVQZ basis set. For the anharmonic treatment, first was calculated the potential surface by displacing the hydrogen and chlorine atoms of HCl. The displacement was from $r - r_o = -0.300$ Å to $r - r_o = 0.800$ Å with a step of 0.025 Å, and after four more points, evenly spaced, were added between $r - r_o = 0.800$ Å and $r - r_o = 1.200$ Å to confirm the potential shape. r denotes the H-Cl distance, and r_o the equilibrium H-Cl distance, for all displacements was taken in account the center of mass of the H-Cl system. For the energies the lowest point energy was also subtracted to simplify calculations as can be seen in Figure 3.

The surface was then used with the variational method to calculate the frequencies using harmonic oscillator and morse oscillator wavefunctions. Unfortunately the morse wavefunctions are highly dependent on $\lambda - 2n - 1$ as can be seen on equation (78), and as our optimized λ was low, that term would become zero or negative really fast which would make the higher n wavefunctions unusable since they wouldn't converge, $\lim_{x\to\infty} \Psi(x) = \infty$. So we weren't able to calculate as much overtone frequencies with the Morse oscillator. These calculations were all made using the Mathematica [82] computational program.

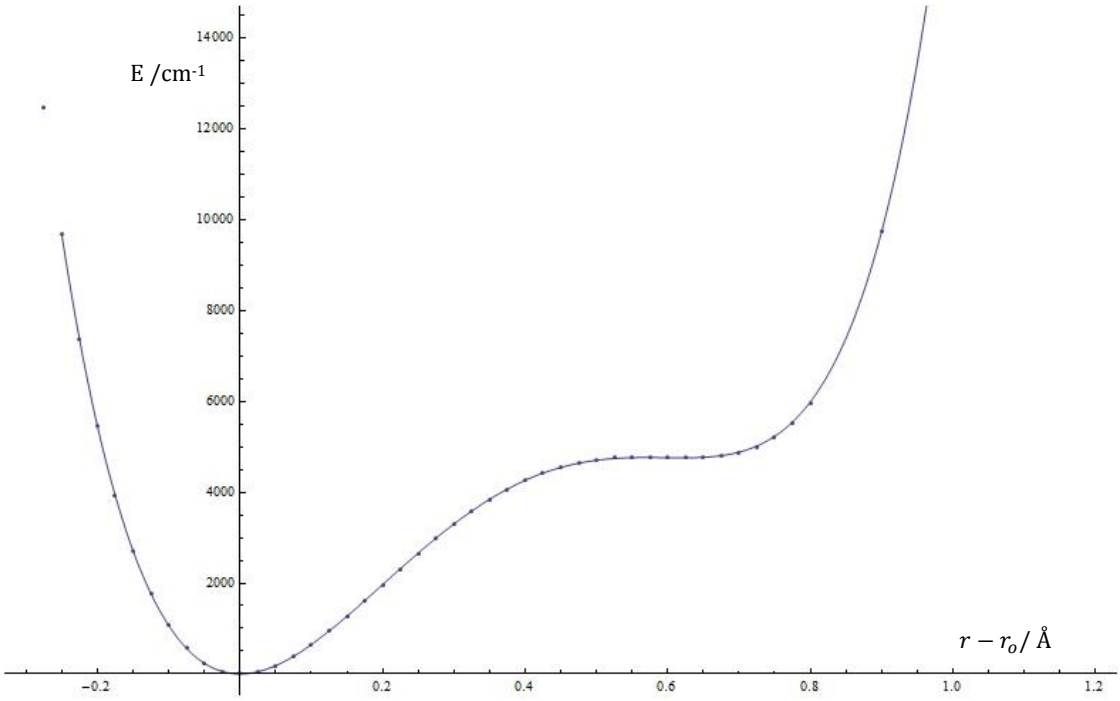

Figure 3 - Potential surface for the H-Cl stretching at CCSD(T)-F12a/AVQZ level.

As we can see in Table 6, the anharmonic contribution is quite important, the harmonic calculations predicted a shift of around 500 cm^{-1} for this stretch in relation to the HCl molecule, while with the anharmonic calculations the predicted shift is of about 800 cm^{-1}. Although the anharmonic treatment does predict a higher shift its still short by about 700 cm^{-1} comparing with the experimental value, which leads us to confirm the presence of matrix effects. Between the Harmonic and Morse oscillator we can see some small differences with fundamental frequency being slightly lower for the Morse oscillator and the overtones slightly higher.

Table 6 - Calculated and experimental frequencies for the H-Cl stretch in the ClH-NH3 complex (in cm^{-1}).

	Δυ=1	Δυ=2	Δυ=3	Δυ=4	Δυ=5
Harmonic Oscillator	2073	3602	4412	5501	6791
Morse Oscillator	2067	3607	4473	—	—
Experimental [77]	1371	—	—	—	—

The next step to refine our results would be checking the existence of coupling between movements to be sure they weren't affecting the experimental values. We started doing that by calculating the potential surfaces for the H-Cl and H-NH_3 stretchings and the H-Cl stretching with Cl-H-N bending. For the later, it was also calculated what would be the energy difference in case the bending was aligned with an ammonia hydrogen or exactly between two of them, and for a 80 degree angle the energy variation was only about 10 cm^{-1}, so an approximation considering cylindrical symmetry was used to simplify calculations. The potential surfaces can be seen in Figure 4. For the bend the angle is calculated between the line that connects the shared hydrogen to the center of mass of the HCl system and the line that connects the nitrogen to the same center of mass.

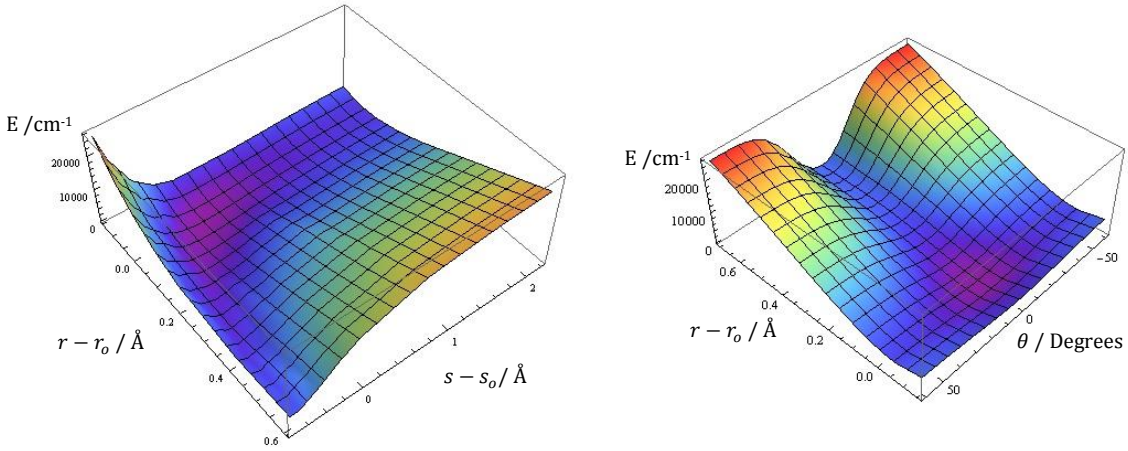

Figure 4 - Potential surfaces for the H-Cl and H-NH_3 stretching (left) and the H-Cl stretching with Cl-H-N bending (right). $\boldsymbol{r}$ is H-Cl distance, $\boldsymbol{s}$ is H-NH_3 distance, $\boldsymbol{\theta}$ is H-(center of mass of HCl)-N angle.

Unfortunately due to time constrains, it wasn't possible to finish the variational calculations for the coupled vibrational frequencies.

4. Conclusions

The ClH-NH_3 complex structure was calculated and optimized with the CCSD(T)-F12a method and the aug-cc-pVQZ basis set. Complex formation keeps the $C_{3\upsilon}$ symmetry from ammonia, and ammonia itself has only very small changes in its structure upon complexation.

In the vibrational modes calculated, the NH_3 symmetric stretch (3481 cm^{-1}) and asymmetric bending (1671 cm^{-1}) show very little change upon complexation, but the lack of experimental data doesn't let us do further observations. The ClH-NH_3 stretch (178 cm^{-1}) has a good agreement with the experimental data. The H-Cl stretch (2390 cm^{-1}) with just harmonic treatment had a difference of about 1000 cm^{-1} between the calculated and the experimental results. Further refinement of that vibrational mode with anharmonic calculations reduced that gap to around 700 cm^{-1} (2073 cm^{-1}), showing its anharmonic treatment is very important and can't be dismissed. To enhance the result a coupling study is proposed, also the introduction of an electric field to simulate the matrix environment could be useful to account for the matrix effects. The NH_3 asymmetric stretch (3613 cm^{-1}) results also show the need for an additional study, introducing anharmonic treatment and/or the electric field can shed some light on the reason for the difference between the experimental and the calculated values, that although not very large, they differ in the direction of the shift upon complexation. The NH_3 symmetric bending (1121 cm^{-1}) mode has a good agreement with the experimental data, both showing an increase in frequency upon complexation, nonetheless it might be possible to get even better results by application of the anharmonic treatment to it. The other calculated vibrational modes are all intermolecular modes and so highly dependent on the position of the hydrogen forming the hydrogen bond, their lack of agreement between the experimental and the calculated can mostly be attributed to the existence of matrix effects.

During the anharmonic treatment we also calculated overtone frequencies that have not been detected experimentally, but we show their values compared to the existing values for the isolated HCl molecule, and as expected they are lower.

In this work the structure is in agreement with previous work. The vibrational modes showed a strong need for anharmonic treatment of this complex and the existence of matrix effects in the experimental data. Also proposes some fine-tuning work that can still be done.

Bibliography

[1] J. H.Seinfeld, *Atmospheric Chemistry and Physics of Air Pollution*, Wiley, 1988.

[2] D. R. Cronn, R. J. Charlson, R. L. Knights, A. L. Crittendon, and B. R. Appel, *Atmos. Environ.*, **11**, 929 (1977).

[3] R. S.Mulliken, *J. Phys. Chem.*, **56**, 801 (1952).

[4] E. Clementi, *J. Chem. Phys.*, **46**, 3851 (1967); *ibid*, **47**, 2323 (1967).

[5] E. Clementi, J. N. and Gayles, *J. Chem. Phys.*, **47**, 3837 (1967).

[6] P. Goldfinger, G. Verhaegen, *J. Chem. Phys.*, **50**, 1467 (1968).

[7] B. S. Ault, and G. C. Pimentel, *J. Phys. Chem.*, **77**, 1649 (1973).

[8] W. Kutzelnigg, and W. Klopper, *J. Chem. Phys.*, **94**, 1985 (1991).

[9] D. P. Tew and W. Klopper, *J. Chem. Phys.*, **123**, 074101 (2005).

[10] A. J. May, E. Valeev, R. Polly, and F. R. Manby, *Phys. Chem. Chem. Phys.*, **7**, 2710 (2005).

[11] S. Ten-no and F. R. Manby, *J. Chem. Phys.*, **119**, 5358 (2003).

[12] T. B. Adler, G. Knizia and H.-J. Werner, *J. Chem. Phys.*, **130**, 1 (2009).

[13] T. B. Adler, G. Knizia and H.-J. Werner, *J. Chem. Phys.*, **127**, 221106 (2007).

[14] T. H. Dunning Jr., *J. Chem. Phys.*, **90**, 1007 (1989).

[15] T. H. Dunning Jr, K. A. Peterson and A. K. Wilson, *J. Chem. Phys.*, **114**, 9244 (2001).

[16] R. A. Kendall and T. H. Dunning Jr., *J. Chem. Phys.*, **96**, 6796 (1992).

[17] B. J. Finlayson-Pitts and J. N. Pitts Jr., *Chemistry of the Upper and Lower Atmosphere*, Academic Press, 2000.

[18] J. H. Seinfeld and S. N. Pandis, *Atmospheric Chemistry and Physics*, John Wiley and Sons, Inc., 2nd ed., 2006.

[19] F. S. Rowland, *Ann. Rev. Phys. Chem.*, **42**, 731 (1991).

[20] S. Solomon, *Nature*, **347** (1990).

[21] R. P. Wayne, *Chemistry of Atmospheres*, 2nd ed., Oxford University Press, 1991.

[22] J. J. Brehms and W. J. Mullin, *Introduction to the Structure of Matter*, John Wiley and Sons, Inc., 1989.

[23] F. Jensen, *Introduction to Computational Chemistry*, John Wiley and Sons, Ltd., 2nd Ed., 2007.

[24] B. T. Sutcliffe, *Adv. Quant. Chem.*, **28**, 65 (1997).

[25] W. Kolos and L. Wolniewicz, *J. Chem Phys.*, **41**, 3663 (1964).

[26] L. J. Butler, *Annu. Rev. Phys. Chem.*, **49**, 125 (1998).

[27] E. F. Valeev and D. C. Sherril, *J. Chem. Phys.*, **118**, 3921 (2002).

[28] N. C. Handy and A. M. Lee, *Chem. Phys. Lett.*, **252**, 425 (1996).

[29] C. C. Roothaan, *Rev. Mod. Phys.*, **23**, 69 (1951).

[30] P. Atkins and R. Friedman, *Molecular Quantum Mechanics*, Oxford University Press, 4th Ed., 2005.

[31] X.-C. Wang, J. Nichols, M. Feyereisen, M. Gutowski, J. Boatz, A. D. J. Haymet and J. Simons, *J. Chem. Phys.*, **95**, 10419 (1991).

[32] T. Van Voorhis and M. Head-Gordon, *J. Chem. Phys.*, **113**, 8873 (2000).

[33] R. J. Bartlett, *J. Chem. Phys.*, **93**, 1697 (1988).

[34] K. Raghavachari, G. W. Trucks, J. A. Pople and M. Head-Gordon, *Chem. Phys. Lett.*, **157**, 479 (1989).

[35] G. E. Scuseria and T. J. Lee, *J. Chem. Phys.*, **93**, 5851 (1990).

[36] T. Helgaker, T. A. Ruden, P. Jørgensen, J. Olsen, and W. Klopper, *J. Phys. Org. Chem.*, **17**, 913 (2004).

[37] A. Halkier, H. Koch, P. Jørgensen, O. Christiansen, I. M. B. Nielsen, and T. Helgaker, *Theor. Chem. Acc.*, **97**, 150 (1997).

[38] T. Helgaker, J. Gauss, P. Jørgensen, and J. Olsen, *J. Chem. Phys.*, **106**, 6430 (1997).

[39] W. Kutzelnigg, *Theor. Chim. Acta*, **68**, 445 (1985).

[40] D. P. Tew, W. Klopper, C. Neiss, and C. Hättig, *Phys. Chem. Chem. Phys.*, **9**, 1921 (2007).

[41] O. Marchetti and H.-J. Werner, *Phys. Chem. Chem. Phys.*, **10**, 3400 (2008).

[42] G. Adler, T. B. Knizia, and H.-J. Werner, *J. Chem. Phys.*, **127**, 221106 (2007).

[43] V. Termath, W. Kutzelnigg and W. Klopper, *J. Chem. Phys.*, **94**, 2002 (1991).

[44] V. Termath, W. Kutzelnigg and W. Klopper, *J. Chem. Phys.*, **94**, 2020 (1991).

[45] F. R. Manby, H.-J. Werner, T. B. Adler and A. J. May, *J. Chem. Phys.*, **124**, 094103 (2006).

[46] H.-J. Werner, T. B. Adler and F. R. Manby, *J. Chem. Phys.*, **126**, 164102 (2007).

[47] G. Knizia and H.-J. Werner, *J. Chem. Phys.*, **128**, 154103 (2008).

[48] C. Hampel, K. A. Peterson and H.-J. Werner, *Chem. Phys. Lett.*, **190**, 1 (1992).

[49] F. R. Manby, *J. Chem. Phys.*, **119**, 4607 (2003).

[50] J. R. Lane and H. G. Kjaergaard, *J. Chem. Phys.*, **131**, 034307 (2009).

[51] G. Rauhut, G. Knizia, and H.-J. Werner, *J. Chem. Phys.*, **130**, 054105 (2009).

[52] J. C. Slater, *Phys. Rev.*, **36**, 57 (1930).

[53] S. F. Boys, *Proc. R. Soc.*, **200**, 542 (1950).

[54] P. Atkins and J. de Paula, *Physical Chemistry*, Oxford University Press, 8th Ed., 2006.

[55] A. Schäfer, H. Horn and R. Ahlrichs, *J. Chem. Phys.*, **97**, 2571 (1992).

[56] A. R. Leach, *Molecular Modelling*, Pearson Education Limited, 2nd Ed., 2001.

[57] F. Jensen, *J. Chem. Phys.*, **122**, 074111 (2005).

[58] K. Jankowski, R. Becheler, P. Scharf, H. Schiffer and R. Ahlrichs, *J. Chem. Phys.*, **82**, 1413 (1985).

[59] A. K. Wilson and T. H. Dunning Jr., *J. Chem. Phys.*, **106**, 88718 (1997).

[60] A. Karton and J. M. L. Martin, *Theor. Chem. Acc.*, **115**, 330 (2006).

[61] R. A. Kendall and T. H. Dunning Jr., *J. Chem. Phys.*, **96**, 6796 (1989).

[62] T. Hrenar, G. Rauhut and H.-J. Werner, *J. Chem. Phys.*, **110**, 2060 (2006).

[63] E. Kauppi and L. Halonen, *J. Chem. Phys.*, **94**, 5779 (1990).

[64] T. Salmi, V. Hänninen, A. L. Garden, H. G. Kjaergaard, J. Tennyson and L. Halonen, *J. Chem. Phys.*, **112**, 6305 (2008).

[65] L. Halonen and T. Carrington Jr., *J. Chem. Phys.*, **88**, 4171 (1987).

[66] E.-J. Kauppi, Ph.D. thesis, University of Helsinki, 1992.

[67] A. Bordoni, Ph.D. thesis, University of Milan, 2006.

[68] L. J. Partanen, MSc thesis, University Of Helsinki, 2011.

[69] R. A. Cazar, A. J. Jamka and F-M Tao, *J. Chem. Phys.*, **102**, 5117 (1998).

[70] S. Saebø, W. Tong and P. Pulay, *J. Chem. Phys.*, **98**, 2170 (1992).

[71] H.-J. Werner, P. J. Knowles, F. R. Manby, M. Schütz, P. Celani, G. Knizia, T. Korona, R. Lindh, A. Mitrushenkov, R. Rauhut, T. B. Adler, R. D. Amos, A. Bernhardson, A. Berning, D. L. Cooper, M. J. O. Deegan, A. J. Bobbyn, F. Eckert, E. Goll, C. Hampel, A. Hesselmann, G. Hetzer, T. Hrenar, G. Jansen, C. Köppl, Y. Liu, A. W. Lloyd, R. A. Mata, A. J. May, S. J. McNicholas, W. Meyer, M. E. Mura, A. Nicklass, P. Palmieri, K. Pflüger, R. Pitzer, M. Reiher, T. Shiozaki, H. Stoll, A. Wolf, MOLPRO, version 2010.1, *A package of ab initio programs*, 2010, see http://www.molpro.net.

[72] E. J. Goodwin, N. W. Howard and A. C. Legon, *Chem. Phys. Lett.*, **131**, 319 (1986).

[73] N. W. Howard and A. C. Legon, *J. Chem. Phys.*, **88**, 4694 (1988).

[74] Z. Latajka, S. Sakai, K. Morokuma and H. Ratajczak, *Chem. Phys. Lett.*, **110**, 464 (1984).

[75] K. P. Huber and G, Herzbert, *Molecular Spectra and Molecular Structure, IV*, Constants of Diatomic Molecules, van Nostrand Reinhold, New York (1979).

[76] R. Hoy, I. M. Mills and G. Strey, *Mol. Phys.*, **24**, 1265 (1972).

[77] A. J. Barnes, T. R. Beech and Z. Mielke, J. Chem. Soc. Far. Trans. II, 80, 455 (1984).

[78] L. S. Rothman, I. E. Gordon, A. Barbe, D. C. Benner, P. F. Bernath, M. Birk, V. Boudon, L. R. Brown, A. Campargue, J. P. Champion, K. Chance, L. H. Coudert, V. Dana, V. M. Devi, S. Fally, J.-M. Flaud, R. R. Gamache, A. Goldman, D. Jacquemart, I. Kleiner, N. Lacome, W. J. Lafferty, J.-Y. Mandin, S. T. Massie, S. N. Mikhailenko, C. E. Miller, N. Moazzen-Ahmadi, O. V. Naumenko, A. V. Nikitin, J. Orphal, V. I. Perevalov, A. Perrin, A. Predoi-Cross, C. P. Rinsland, M. Rotger, M. Šimečková, M. A. H. Smith, K. Sung, S. A. Tashkun, J. Tennyson, R. A. Toth, A. C. Vandaele and J. Vander Auwera, *J. Quant. Spectrosc. Radiat. Transf.*, **110**, 533 (2009).

[79] G. Corongiu, D. Estrin, G. Murgia, L. Paglieri, L. Pisani, G. S. Valli, J.D. Watts and Clementi, E., *Int. J. Quantum Chem.*, **59**, 119 (1996).

[80] M. M. Szczęśniak, I. J. Kurnig and S. Scheiner, *J. Phys. Chem.*, **89**, 3131 (1992).

[81] Y. Bouteiller, C. Mijoule, A. Karpfen, H. Lischka and P. Schuster, *J. Phys. Chem.*, **91**, 4464 (1987).

[82] Wolfram Research, Inc., *Mathematica Edition: Version 8.0*, Wolfram Research, Inc., 2010.